치의과학박사 학위논문

# Preclinical comparative evaluation of zirconia crowns based on manufacturing methods and materials

## 제조 방식 및 재료에 따른 지르코니아 보철물의 전임상 비교 연구

2023년 2월

서울대학교 대학원

치의과학과 치과보철학 전공

김 용 규

# Preclinical comparative evaluation of zirconia crowns based on manufacturing methods and materials

지도교수 한 중 석

이 논문을 치의과학박사 학위논문으로 제출함
2022년 12월

서울대학교 대학원
치의과학과 치과보철학 전공
김 용 규

김용규의 치의과학박사 학위논문을 인준함
2023년 1월

위 원 장 _____ 윤 형 인 _____ (인)

부위원장 _____ 한 중 석 _____ (인)

위　　원 _____ 여 인 성 _____ (인)

위　　원 _____ 임 범 순 _____ (인)

위　　원 _____ 김 형 섭 _____ (인)

# ABSTRACT

# Preclinical comparative evaluation of zirconia crowns based on manufacturing methods and materials

Yong-Kyu Kim, D.D.S., M.S.D.

Program in Prosthodontics, Department of Dental Science,

Graduate School, Seoul National University

(Directed by Prof. Jung-Suk Han, D.D.S., M.S., Ph.D.)

***Purpose.*** This study aimed to comparatively analyze several single-unit zirconia prostheses fabricated using various manufacturing methods and materials with the intaglio surface trueness, antagonist's wear volume loss, and fracture resistance at the preclinical stage.

***Materials and methods.*** A total of 7 experimental groups was included: Two additive manufacturing zirconia groups with different stereolithography (SLA) and digital light processing (DLP) printers, a fully sintered zirconia ((Y, Nb)-stabilized zirconia) group, and four groups of 4 or 5 mol% yttria-stabilized partially sintered zirconia by conventional or speed sintering. For each group, 14 monolithic zirconia crowns were made. Using 3D inspection software, the intaglio surface trueness was

assessed at the inner surface, occlusal, margin, and axial areas after the specimen had been scanned with an intraoral scanner. Half of the specimens were aged for 120,000 cycles in the chewing simulator with human molars as antagonists. Each antagonist was digitized by a laboratory scanner before and after the chewing cycle. Volume loss was calculated by superimposing each pair of scan data using 3D inspection software. For all specimens, the load value at the time of fracture was evaluated using a universal testing machine. The trueness values were assessed with Welch's ANOVA, and the wear volume loss was assessed with the Kruskal–Wallis tests. The effect of the zirconia group and aging on fracture resistance of crowns was investigated using two-way ANOVA. The one-way ANOVA was used to assess the difference between groups in fracture load values before and after aging, respectively. A paired t-test was used to investigate the effect of aging on the fracture load for each group.

***Results.*** There were significant differences in trueness between the groups, but the variations in mean of root mean square were within 5.25 μm. The two additive manufactured groups showed high trueness and low variations in the axial and occlusal areas but low trueness in the marginal area. The intaglio surface of the FSZ group was more reproducible than the partially sintered zirconia group but showed lower trueness in the occlusal and marginal areas. The partially sintered zirconia groups had low trueness in the axial area. There was no significant difference due to speed sintering on identical partially sintered zirconia blocks. No zirconia fractures were observed in any group during the artificial aging, and the amount of zirconia wear could not be detected. In wear volume loss of antagonists, there were no substantial variations among the ($p = 0.808$). Both zirconia groups

and artificial aging had statistically significant effects on fracture load (both, $p < 0.001$), but no interaction between groups and aging was found ($p = 0.301$). The ADZ and FSZ groups had significantly higher fracture load values than others both before and after aging. Due to aging, only the fracture load values of the S4Z, C4Z, and C5Z groups decreased significantly.

***Conclusion.*** Full-contour crowns made of additive manufactured zirconia, fully sintered zirconia, and partially sintered zirconia are clinically acceptable, with showing satisfactory results in intaglio surface trueness, antagonist's wear volume loss, and fracture resistance after artificial aging.

---

**Keyword :** Zirconia; Additive manufacturing; Fully-sintered zirconia; Speed sintering; Intaglio surface trueness; Fracture resistance; Artificial aging

**Student Number :** 2019-39896

# CONTENTS

# 1. INTRODUCTION

With advancements in computer-aided design and computer-aided manufacturing (CAD/CAM) technologies, zirconia ceramic has become the preferred material for dental prostheses, due to its excellent biocompatibility and mechanical properties (Gautam et al, 2016). The early generations of zirconia (3 mol% yttria-stabilized tetragonal zirconia polycrystal, 3Y-TZP) have excellent physical properties because of transformation toughening, where the volume expands by 3%–5% during the martensitic transformation (Denry and Kelly, 2008, Stawarczyk et al, 2017, Miyazaki et al, 2013) However, it has less translucency than glass-ceramics (Denry and Kelly, 2008, Stawarczyk et al, 2017). New generations of dental zirconia (4 or 5 mol% yttria partially stabilized zirconia, 4Y- or 5Y-PSZ) have been developed with a higher cubic content, resulting in better translucency but poorer physical properties (Stawarczyk et al, 2017, Kolakarnprasert et al, 2019). This zirconia can be used as a monolithic and fully anatomic form in esthetically demanding areas, resolving porcelain veneer chipping (Stawarczyk et al, 2017, Kolakarnprasert et al, 2019, Malkondu et al, 2016).

In fabricating CAD/CAM zirconia dental prostheses, the 4- or 5-axis milling techniques are widely used to fully or partially sintered zirconia blocks because of their reproducibility and accuracy (Abduo et al, 2010, Att et al, 2009). Zirconia prostheses are typically milled from pre-sintered blocks to reduce tool wear and phase transformation, resulting in white-stage specimens that require

final sintering (Denry and Kelly, 2008). However, becausethe conventional sintering protocol takes 4–12 hours to complete, it is time consuming, so speed or high-speed sintering has recently gained attention as a possible alternative (Jansen et al, 2019, Antón et al, 2021, Wiedenmann et al, 2020). By high-speed sintering, the accuracy of the crown was not markedly affected (Jansen et al, 2019, Antón et al, 2021), but the transparency decreased, and the fracture load remained constant or increased (Wiedenmann et al, 2020). This is because zirconia ceramics' temperature, holding time, and total sintering time all impacted their optical and mechanical properties (Stawarczyk et al, 2013).

The fully sintered block is another option that saves sintering time and can be delivered in a single visit (Cho et al, 2019). Fully sintered zirconia has a lower volume proportion of pores, higher strength, and more precise fitting than partially sintered zirconia (Ahmed et al, 2019b). However, when milling, fully sintered zirconia blocks have a more rigid surface than partially sintered zirconia blocks, which may result in increased tool wear (Cho et al, 2019, Tinscherta et al, 2004). A fully sintered (Y, Nb)-TZP block with a low surface hardness has been developed to address these concerns. (Y, Nb)-TZP is a modified tetragonal zirconia solid solution comprising $Y_2O_3$ and $Nb_2O_5$ (Kim et al, 2013). It has excellent machining capability and has little phase transformation during processing because of stabilizers like Nb (Jeong et al, 2021, Kim et al, 2000).

However, these subtraction manufacturing (SM) methods are difficult to reproduce the complex shape and have various manufacturing limitations, including fine cracks on the ceramic surface caused by milling and tool wear (Van Noort, 2012, Schriwer et al, 2017). Furthermore, the remainder of the zirconia block after milling may be discarded following the fabrication process (Strub et al,

2006, Khanlar et al, 2021). The additive manufacturing (AM) of zirconia has been investigated to address the shortcomings of subtractive manufacturing (Khanlar et al, 2021). AM methods are expected to produce complex geometries while reducing production time and waste (Torabi et al, 2015, Schwentenwein and Homa, 2015, Ebert et al, 2009). Among the various AM methods for ceramics, vat polymerization methods such as stereolithography (SLA) and digital light processing (DLP) are the most appropriate strategy for digital dental workflows because of their precision (Wang and Sun, 2021). The UV laser in the SLA 3D printer cures the photo-curable liquid resin. Each layer is laminated and cured point by point, resulting in precise output and excellent surface roughness (Dikova et al, 2018). The DLP 3D printer irradiates and laminates each layer by face unit one at a time, resulting in more accurate output and a shorter production time (Dikova et al, 2018). The strength of additive manufactured ceramic crowns was comparable to subtractive manufactured crowns and accuracy was reported to be within the clinically acceptable range (Wang and Sun, 2021, Wang et al, 2019, Li et al, 2021, Lerner et al, 2021, Revilla-León et al, 2020, Stawarczyk et al, 2017, Kolakarnprasert et al, 2019, Malkondu et al, 2016). The slurry composition, heat treatment schedules, layer thicknesses, light strategies, and other parameters may impact the characteristics of additive manufactured ceramic objects (Revilla-León et al, 2021, Ioannidis et al, 2020).

Multiple factors must be considered to produce a clinically successful zirconia prosthesis over the long term. For proper prosthesis seating, accurate fabrication of the inner surface is required. If not properly seated, the cement layer can become anomalously thick, resulting in residual stresses on the tensile surface (Kirsch et al, 2017, Bindl and Mörmann, 2007, Rekow and Thompson, 2005).

Furthermore, marginal misfit increases plaque retention with secondary caries and can lead to periodontal disease (Sailer et al, 2007, Lang et al, 1983, Felton et al, 1991, Goldman et al, 1992). Accuracy is generally measured in two ways: trueness and precision. Precision conveys measurement values' proximity, while trueness reflects how close measurement values are to true value (Mehl et al, 2021). Fracture resistance is another major factor in clinical applications that must withstand occlusal forces (Scherrer and De Rijk, 1993). Material properties, crown thickness, and shape impact the fracture resistance of all ceramic crowns (Scherre and De Rijk, 1992, Nakamura et al, 2015). Furthermore, clinical failure of all ceramic restorations is a highly complex process involving patient variables, dynamic loading, and fatigue (White et al, 2005). Therefore, it is necessary to investigate the properties of prostheses in cases prone to cyclic fatigue (Wiskott et al, 1995, Wiedenmann et al, 2020). Fatigue failure is defined as the formation of subcritical cracks in pre-existing flaws due to intermittent stress below the material's specific fracture strength in an aqueous environment (Liu and Chen, 1991). In particular, zirconia materials are linked with susceptibility to hydrothermal aging, a process in which water molecules cross grain boundaries (Chevalier et al, 2007, Lümkemann and Stawarczyk, 2021). The consequences of hydrothermal aging are surface roughening, increased wear rates, mechanical property loss, and even catastrophic failure (Camposilvan et al, 2018, Zhang et al, 2016). Many factors, such as different grain sizes, density, the $Y_2O_3$ content in the tetragonal phase, and cubic phase proportion, all contribute to the aging process (Wei and Gremillard, 2018).

This study aimed to assess the intaglio trueness, wear of antagonists, and fracture resistance to confirm the clinical use of zirconia prostheses made using

AM, fully sintered zirconia, and speed sintering. The first research hypothesis stated that there would be no difference in the intaglio trueness of the crowns regardless of manufacturing methods. The second research hypothesis proposed that the wear volume loss of antagonistic teeth would be comparable regardless of the manufacturing method. The third research hypothesis was that no difference in the fracture resistance would be found between the differently manufactured zirconia groups, regardless of artificial aging.

# 2. MATERIAL and METHODS

## 2.1. Specimen preparation

The tooth reduction (occlusal: 1.5 mm, axial: 1–1.5 mm, chamfered margin: 1 mm, rounded extension angle) was conducted on mandibular first molars, using standardized acrylic resin teeth (Simple Root Tooth Model; Nissin Dental Products, Kyoto, Japan). The prepared resin tooth was digitized with less than 7-micron accuracy using a laboratory scanner (T500; Medit, Seoul, Korea). Ninety-eight metal abutments were made of powdered CoCr alloys (SP2 CoCr; Eos GmbH, Krailling, Germany) using the direct metal laser sintering technique (EOSINT M270; Eos GmbH, Krailling, Germany). A full-contour monolithic crown was created on the prepared die using dental CAD software (Dental Designer; 3Shape, Copenhagen, Denmark), with a cementation space of 25 μm beginning at a distance of 1 mm from the margin.

The crowns were divided into seven groups, with each group receiving 14 specimens. (1) Group 1 (ADZ) was additive manufactured zirconia using a 3Y-TZP zirconia suspension (M.O.P., Kyunggi-do, Korea) — zirconium dioxide, hexamethylene diacrylate, polyethylene glycol diacrylate, TPO — fabricated by DLP format 3D printer (Octave Light R1; Octave Light Limited, Shatin, N.T., Hong Kong). Debinding and sintering were conducted under the manufacturer's recommendations. (2) Group 2 (ASZ) was additive manufactured zirconia using a 3Y-TZP zirconia suspension (3D Ceram, Limoges, France) — AIN, 3Y-zirconia,

8Y-zirconia, silicon nitride, alumina toughened zirconia, silica — fabricated by SLA format 3D printer (C100 EASY; 3D Ceram, Limoges, France). Debinding and sintering were conducted following the manufacturer's recommendations. (3) Group 3 (FSZ) was fully sintered Y, Nb zirconia group (Perfit FS; vatech mcis, Gyeonggi-do, Korea). It was manufactured using dental CAM software (Millbox; CIM system, Milano, Italy) and a 4-axis wet milling machine (Cori TEC one; imes-icore, Eiterfeld, Germany). (4) Group 4 (C4Z) was partially sintered 4Y-PSZ zirconia group (KATANA STML; Kuraray Noritake Dental Inc, Tokyo, Japan) made using dental CAM software (HyperDent; Follow-me! Technology, Munich, Germany) and a 5-axis milling machine (Arum 5X-300; Doowon, Daejeon, Korea). Following milling, sintering was conducted for 7 hours under the manufacturer's instructions. (Heated at a rate of 10℃/min for 2 hours 30 minutes, maintained at 1550℃ for 2 hours, and then cooled at a rate of −10℃/min for 2 hours 30 minutes.). (5) Group 5 (S4Z) was manufactured using the same zirconia disc and laboratory system as the C4Z group. Following milling, sintering was performed for 90 minutes alternately according to the manufacturer's instructions (Heated at a rate of 35℃/min for 45 minutes, maintained at 1560–1565℃ for 30 minutes, and then cooled at a rate of -45℃/min for 15 minutes.). (6) Group 6 (C5Z) was made of partially sintered 5Y-PSZ zirconia (KATANA UTML; Kuraray Noritake Dental Inc, Tokyo, Japan). It was manufactured using the same laboratory system and sintering process as the C4Z group. (7) Group 7 (S5Z) was manufactured using the same zirconia disc and laboratory system as the C5Z group. The S4Z group implemented the sintering schedule in the same way. The process of subsequent experiments is summarized in Figure 1.

## 2.2. Intaglio surface trueness

The intaglio surfaces were scanned using an intraoral scanner (i500; Medit, Seoul, Korea) with an in vitro precision of 5μm. Because the scan angle and distance slightly limited the laboratory scanner's digitization procedure to the crown's intaglio surfaces, the intraoral scanner was used after thorough calibration and adjustment according to the manufacturer's instructions. The scanning procedure was conducted in the absence of natural light. Calibration was conducted following the manufacturer's instructions at each stage of the specimen scanning procedure. Each scan data of the intaglio surface of the zirconia crown was superimposed on the internal area of the virtual crown from the CAD file (reference data) using the 3D inspection software (Geomagic Control X; Geomagic Inc, Morrisville, NC, USA). After defining the internal area of the virtual crown as the region of interest, the best-fit alignment was performed using an iterative closest point algorithm, based on point-to-point measurements. Trueness indicates the degree of closeness between the measurement value and the true value. To compare the trueness of the inner surface of crowns, the root mean square (RMS) value between scan data and reference data was calculated at the four inspection regions: inner surface, occlusal, margin, and axial area. The color deviation map was also provided. A single investigator scanned and superimposed each crown specimen.

## 2.3. Artificial aging and wear volume loss

Half of the specimens (n = 7 for each group) were cemented onto a metal abutment with self-curing resin cement (RelyX-U200; 3M-ESPE, St. Paul, MN, USA) for thermal cycling and mechanical loading. The specimens were artificially aged in a chewing simulator (Chewing Simulator CS-4.8; SD Mechatronik, Feldkirchen-Westerham, Germany). Forty-nine human maxillary molars were employed as antagonists. These biospecimens were provided by the Biobank of Seoul National University Dental Hospital, a member of the Korea Biobank Network (KBN4_A04). The donor's personal information was anonymized so that the researcher could not know, and therefore IRB review was exempted (IRB Number: ERI21022).

Only the disto-palatal cusps were opposed after the other cusps were modified with a diamond bar (Dia-Burs EX-21F; MANI, Tochigi, Japan). These were embedded in self-curing acrylic resin (Vertex Self-Curing; Vertex Dental, Soesterberg, Netherlands) and to act as enamel antagonists. The specimen was mechanically loaded with 50 N at 1.5 Hz for 1,200,000 cycles. Simultaneous thermal cycling in water was accomplished by varying the temperature from 5℃ to 55℃ every 60s. A 0.7 mm sliding movement from the central fossa to the buccal cusp was conducted. The 1.2 million dynamic loading cycles with thermal cycling between 5–55℃ were performed, which is equivalent to 5 years of clinical service (DeLong and Douglas, 1991, Steiner et al, 2009). Table 1 lists the thermal cycling and mechanical loading parameters used in this study. Each antagonist was dried and digitized with fewer than 7-micron accuracy by a laboratory scanner (T500;

Medit, Seoul, Korea) before and after the chewing cycle. Using 3D inspection software (Geomagic Control X; Geomagic Inc, Morrisville, NC, USA), each pair of scan data was superimposed to compute the volume loss ($mm^3$).

## 2.4. Fracture resistance

The remaining specimens were cemented onto metal abutments using self-curing resin cement (RelyX-U200; 3M-ESPE, St. Paul, MN, USA). All specimens' fracture resistance was evaluated using a universal testing machine (Instron 8871; Instron, Norwood, MA, USA). A 5 mm diameter stainless-steel spherical indenter was employed to contact the central fossa of each crown. A 2 mm urethane sheet was placed on the occlusal surface to prevent excessive local force. Compressive loading was performed at 0.5 mm/min crosshead speed using a 10 kN load cell until fracture occurred, at which point the load (N) at failure was recorded.

## 2.5. Statistical analysis

The means and standard deviations of the trueness measurements (RMS value, μm), the fracture load values (N), and the amount ($mm^3$) of volume loss of the antagonists for each group were measured. Because the RMS data satisfy the assumption of normality but contravene the equality of variances, Welch's analysis of variance (ANOVA) was performed, followed by post-hoc validation using the

Games–Howell test. Because of the small sample size, the antagonist volume loss was confirmed statistically using the Kruskal–Wallis test. The impact of two factors on fracture resistance was investigated using a two-way ANOVA: manufacturing procedures and artificial aging, as well as their interactions. One-way ANOVA was used to establish whether there was a disparity in fracture load values between groups before and after aging, respectively, and post-hoc validation was performed using Bon Ferroni's correction. Finally, a paired t-test was used to assess whether the fracture load values varied for each group before and after aging. Statistical software (IBM SPSS Statistics v26.0; IBM Corp., Armonk, NY, USA) was employed for all analyses, with a statistical significance threshold (p) of 0.05.

# 3. RESULTS

## 3.1 Intaglio surface trueness

The mean and standard deviation of RMS are summarized in Table 2, and the statistical significance of each group using Welch's ANOVA is shown in Figure 2. In Figure 3, the color deviation maps showed that most of the inner surfaces of the evaluated crowns had green areas, indicating surface deviation within 50 μm. In the entire inner surface area, ASZ had the highest mean RMS (34.81 μm) with a significant difference between the three groups, and S4Z had the lowest mean RMS (26.94 μm) with a significant difference between the two groups. C4Z had the highest standard deviation (9.10 μm), while ADZ had the lowest (1.30 μm). Other partially zirconia groups also had a high deviation (3.63–5.91 μm).

In the margin area, the RMS values of ADZ and ASZ were significantly higher than the other groups. The ASZ had the highest mean RMS value (62.39 μm), but there was no significant difference between it and ADZ (54.20 μm). However, the standard deviation of ADZ was 5.08 μm, which was greater than that of ASZ (3.08 μm). The mean value of FSZ demonstrated the next largest (37.96 μm) which was significantly different from the three partially sintered zirconia groups. The C5Z group had the highest standard deviation (8.85 μm), while the ASZ group had the lowest variance (3.08 μm).

In the occlusal area, FSZ had the highest mean RMS value (29.81 μm) with a significant difference from the other four groups, while the ADZ group had the

lowest mean RMS value (19.47 μm) with a significant difference from the other two groups. C4Z had the highest standard deviation (4.75 μm) and ASZ had the lowest (2.49 μm). In the axial area, FSZ had the highest mean RMS value (36.69 μm), while ASZ had the lowest observed value (21.51 μm). In terms of standard deviation, partially sintered zirconia groups generally had high RMS, with C4Z having the highest (14.78 μm) and ADZ having the lowest (3.90 μm).

## 3.2 Wear volume loss

No zirconia fractures were found during the artificial aging, and the amount of zirconia wear was relatively minimal. The wear volume losses of the antagonist after 120,000 cycles were 2.06 ± 1.24, 1.74 ± 1.20, 1.49 ± 1.58, 2.51 ± 2.13, 2.49 ± 1.33, 2.40 ± 1.66, and 2.05 ± 1.24 $mm^3$ for Groups ADZ, ASZ, FSZ, C4Z, S4Z, C5Z, S5Z, in that order. Kruskal–Wallis test revealed no significant difference between the groups ($p = 0.808$).

## 3.3 Fracture resistance

Table 3 and Figure 4 displays the means and standard deviations of the fracture load values (N) for all groups. Two-way ANOVA showed that both zirconia groups and artificial aging had statistically significant impacts on the value of fracture load (both, $p < 0.001$). There was no interaction between groups and

aging ($p = 0.301$). When comparing groups before aging by one-way ANOVA, the ADZ and FSZ groups had significantly higher values than the other groups. There was also a significant difference between the ASZ and 5SZ groups. In the results after aging, ADZ and FSZ also had significantly higher values than the other groups. The speed sintering group demonstrated a lower fracture load value, but not more significant than the conventional sintering group. When a significant change in fracture load value due to aging was observed for each group via paired t-tests, only the S4Z, C4Z, and C5Z groups revealed a significant decrease. In all other groups, although not statistically significant, fracture load values declined due to aging.

# 4. DISCUSSION

The two AM groups outperformed the other groups in terms of better trueness and less variation in the axial and occlusal regions. In the other groups fabricated by the subtractive method, accuracy can be reduced when the diameter of the bur is larger than the radius of curvature of the abutment, particularly in axial to occlusal transitions (Kirsch et al, 2017). However, AM groups demonstrated low margin trueness. It is possible to consider it because the surface of the additive manufactured zirconia has a stepped shape, which reduces the trueness in the line angle or marginal area (Wang and Sun, 2021, Revilla-León et al, 2020). Furthermore, because the green structure immediately after the following printing has weak physical properties, thin areas are vulnerable to damage during physical handling and subsequent post-processing, debinding, and sintering (Li et al, 2021). Among the two AM groups, ADZ demonstrated better trueness except for the axial area. In general, differences in the accuracy of printed objects have been attributed to various ceramic slurries, light sources, and machines rather than the technologies themselves (Wang et al, 2019, Revilla-León et al, 2020, Son et al, 2021).

The FSZ group's intaglio surface was more reproducible than the partially sintered zirconia groups. Partially sintered zirconia prostheses may experience non-uniform shrinkage after sintering, resulting in relatively large deviations when compared to fully sintered zirconia prostheses (Rezende et al, 2017, Schriwer et al, 2017). The FSZ group, however, had the lowest trueness and the greatest variance in the occlusal area. In this study, the FSZ was made with 4-axis milling, and the

accuracy is lower than with 5-axis milling, especially in deep areas and occlusal angles (Cho et al, 2019, Alghazzawi, 2016). FSZ also had low trueness in the margin area, probably because it is more brittle when milled, resulting in poor accuracy in thin sections (Abduo et al, 2010).

There was no distinction in trueness due to speed sintering in the same zirconia blocks. In previous studies, prostheses made by high-speed sintering demonstrated similar accuracy to conventional sintering (Ahmed et al, 2019a) or were more inaccurate due to varying patterns of temperature change and sintering shrinkage (Antón et al, 2021, Kauling et al, 2020, Nakamura et al, 2020). The C4Z group had a relatively large variance, particularly in the axial area, which is only considered an error due to bur wear or careless handling during production.

There was no significant difference in antagonist wear between groups, but FSZ was minimal, followed by the smallest AM groups. Ceramic-induced enamel wear is more important to surface roughness and microstructure than hardness (Oh et al, 2002). Furthermore, internal porosity and other surface defects caused by an insufficient firing technique act as stress concentrators, resulting in increased wear (Oh et al, 2002). The fact that FSZ showed relatively little wear is thought to be due to fewer defects on the inner surface as a result of well-controlled fully sintering. The roughness of additive manufactured zirconia may increase further due to the surface's step shape (Janyavula et al, 2013, Wang et al, 2019), but this does not appear to have a significant effect.

The fracture resistance of ADZ was higher than that of ASZ, which exhibited characteristics similar to the 4YZ groups. The zirconia slurry of the two AM groups appeared to have better fracture resistance than the other groups because it was primarily composed of 3Y-TZP, but there was a difference between

the two groups. Differences in slurry composition and debinding rates may have impacted the fracture resistance of the printed objects (Ioannidis et al, 2020, Revilla-León et al, 2021). Furthermore, variations in layer thickness, light source, and polymerization strategies may have resulted in variations in the formation or distribution of micro-level pores, which may have affected fracture resistance(Revilla-León et al, 2021, Ioannidis et al, 2020). Because the manufacturing strategy used in this study is unknown, comparative experiments to control for these factors are required. FSZ had the highest failure load value after ADZ. To enhance the machinability of zirconia, low hardness and high fracture toughness are required (Pyo et al, 2020). Therefore, the FSZ made of zirconia with improved machinability demonstrated a high failure load. Speed sintering in partially sintered zirconia groups aggravated fracture resistance, although not significantly. Previous research found that zirconia crowns subjected to high-speed sintering had smaller grain sizes and higher fracture resistance than conventional sintering (Jansen et al, 2019, Wiedenmann et al, 2020). However, some studies found that the fracture load values did not change due to speed sintering (Nakamura et al, 2020, Michailova et al, 2020, Kauling et al, 2020).

AM groups were less influenced by artificial aging. The higher the stabilizer content, such as yttria, the more cubic zirconia appears in the microstructure, reducing the phase transition and making it more resistant to aging (Pereira et al, 2018, Rezende et al, 2017, Camposilvan et al, 2018, Zhang et al, 2016), but AM groups using 3Y-TZP slurry did not. Low-temperature degradation is driven by the annihilation of oxygen vacancies, which alumina can stabilize (Schubert and Frey, 2005, Wei et al, 2020). Therefore, the alumina content of the polycrystalline structure influences the aging behavior of the zirconia groups tested.

FSZ demonstrated a relatively mild change in strength due to artificial aging. This is primarily due to the Y-Nb alignment's phase stability (Kim et al, 2000). Only the 4YZ and 5YZ groups were influenced by artificial aging, most likely because the stabilizing factors in the other group were more functional.

This in vitro study has some limitations. First, variables in AM could not be controlled, such as variations in printing mechanism, printing conditions, parameters, and slurry composition. Because shrinkage rates in additive and subtractive manufacturing differ depending on geometric shape (Revilla-León et al, 2020), more research comparing different types of prostheses is required. It would have been preferable to include the 3Y-TZP milling group, which is similar to the AM group in composition. Furthermore, using Co–Cr alloy for testing abutments with high elastic modulus may result in a relatively high fracture load value (Scherrer and De Rijk, 1993). It appears that a situation similar to the clinical situation is required. Finally, because the zirconia blocks of partially sintered zirconia groups were manufactured by the same company, the results cannot be generalized. It would be necessary to investigate various manufacturers' impact on materials and milling conditions.

# 5. CONCLUSION

Within the limitation of this study, additive manufacturing produced a strong and accurate zirconia prosthesis, excluding the margin with the possibility of compensating for the shortcomings of subtractive manufacturing. Fully-sintered (Y, Nb)-TZP showed higher reproducibility and applicability in the posterior teeth. In partially sintered zirconia, Speed sintering produced a clinically functional prosthesis similar to conventional sintering.

# REFERENCES


ABDUO, J., LYONS, K. & SWAIN, M. Fit of zirconia fixed partial denture: a systematic review. *Journal of Oral Rehabilitation*. 2010;37(11):866-876.

AHMED, W. M., ABDALLAH, M. N., MCCULLAGH, A. P., WYATT, C. C., TROCZYNSKI, T. & CARVALHO, R. M. Marginal discrepancies of monolithic zirconia crowns: The influence of preparation designs and sintering techniques. *Journal of Prosthodontics*. 2019a;28(3):288-298.

AHMED, W. M., TROCZYNSKI, T., MCCULLAGH, A. P., WYATT, C. C. & CARVALHO, R. M. The influence of altering sintering protocols on the optical and mechanical properties of zirconia: a review. *Journal of Esthetic and Restorative Dentistry*. 2019b;31(5):423-430.

ALGHAZZAWI, T. F. Advancements in CAD/CAM technology: Options for practical implementation. *Journal of Prosthodontic Research*. 2016;60(2):72-84.

ANTóN, X., STAWARCZYK, B., REYMUS, M., JODA, T. & LIEBERMANN, A. Impact of High-Speed Sintering on Accuracy and Fit of 4 mol% Yttria-Stabilized Tetragonal Zirconia Polycrystals. *International Journal of Prosthodontics*. 2021;34(6):775-783.

ATT, W., KOMINE, F., GERDS, T. & STRUB, J. R. Marginal adaptation of three different zirconium dioxide three-unit fixed dental prostheses. *The Journal of Prosthetic Dentistry*. 2009;101(4):239-247.

BINDL, A. & MöRMANN, W. H. Fit of all-ceramic posterior fixed partial denture frameworks in vitro. *International Journal of Periodontics & Restorative*

*Dentistry*. 2007;27(6):566-575.

CAMPOSILVAN, E., LEONE, R., GREMILLARD, L., SORRENTINO, R., ZARONE, F., FERRARI, M. & CHEVALIER, J. Aging resistance, mechanical properties and translucency of different yttria-stabilized zirconia ceramics for monolithic dental crown applications. *Dental Materials*. 2018;34(6):879 -890.

CHEVALIER, J., GREMILLARD, L. & DEVILLE, S. Low-temperature degradation of zirconia and implications for biomedical implants. *Annual Review of Materials Research*. 2007;37:1-32.

CHO, J. H., YOON, H. I., HAN, J. S. & KIM, D. J. Trueness of the Inner Surface of Monolithic Crowns Fabricated by Milling of a Fully Sintered (Y, Nb)-TZP Block in Chairside CAD–CAM System for Single-visit Dentistry. *Materials*. 2019;12(19):3253.

DELONG, R. & DOUGLAS, W. H. An artificial oral environment for testing dental materials. *IEEE Transactions on Biomedical Engineering*. 1991;38(4):339-345.

DENRY, I. & KELLY, J. R. State of the art of zirconia for dental applications. *Dental Materials*. 2008;24(3):299-307.

DIKOVA, T., DZHENDOV, D., IVANOV, D. & BLIZNAKOVA, K. Dimensional accuracy and surface roughness of polymeric dental bridges produced by different 3D printing processes. *Archives of Materials Science and Engineering*. 2018;94(2): 65-75.

EBERT, J., ÖZKOL, E., ZEICHNER, A., UIBEL, K., WEISS, Ö., KOOPS, U., TELLE, R. & FISCHER, H. Direct inkjet printing of dental prostheses made of zirconia. *Journal of Dental Research*. 2009;88(7):673-676.

FELTON, D., KANOY, B., BAYNE, S. A. & WIRTHMAN, G. Effect of in vivo crown margin discrepancies on periodontal health. *The Journal of Prosthetic Dentistry*. 1991;65(3):357-364.

GAUTAM, C., JOYNER, J., GAUTAM, A., RAO, J. & VAJTAI, R. Zirconia based dental ceramics: structure, mechanical properties, biocompatibility and applications. *Dalton Transactions*. 2016;45(48):19194-19215.

GOLDMAN, M., LAOSONTHORN, P. & WHITE, R. R. Microleakage—full crowns and the dental pulp. *Journal of Endodontics*. 1992;18(10):473-475.

IOANNIDIS, A., BOMZE, D., HäMMERLE, C., HüSLER, J., BIRRER, O. & MüHLEMANN, S. Load-bearing capacity of CAD/CAM 3D-printed zirconia, CAD/CAM milled zirconia, and heat-pressed lithium disilicate ultra-thin occlusal veneers on molars. *Dental Materials*. 2020;36(4):e109-e116.

JANSEN, J. U., LüMKEMANN, N., LETZ, I., PFEFFERLE, R., SENER, B. & STAWARCZYK, B. Impact of high-speed sintering on translucency, phase content, grain sizes, and flexural strength of 3Y-TZP and 4Y-TZP zirconia materials. *The Journal of Prosthetic Dentistry*. 2019;122(4):396-403.

JANYAVULA, S., LAWSON, N., CAKIR, D., BECK, P., RAMP, L. C. & BURGESS, J. O. The wear of polished and glazed zirconia against enamel. *The Journal of Prosthetic Dentistry*. 2013;109(1):22-29.

JEONG, K. W., YOON, H. I., LEE, J. H., YEO, I. S. L., KIM, D. J. & HAN, J. S. Clinical Feasibility of Fully Sintered (Y, Nb)-TZP for CAD-CAM Single-Unit Restoration: A Pilot Study. *Materials*. 2021;14(11):2762.

KAULING, A. E., GüTH, J. F., ERDELT, K., EDELHOFF, D. & KEUL, C. Influence of speed sintering on the fit and fracture strength of 3-unit

monolithic zirconia fixed partial dentures. *The Journal of Prosthetic Dentistry*. 2020;124(3):380-386.

KHANLAR, L. N., SALAZAR RIOS, A., TAHMASEB, A. & ZANDINEJAD, A. Additive manufacturing of zirconia ceramic and its application in clinical dentistry: a review. *Dentistry Journal*. 2021;9(9):104.

KIM, D. J., LEE, M. H., LEE, D. Y. & HAN, J. S. Mechanical properties, phase stability, and biocompatibility of (Y, Nb)-TZP/$Al_2O_3$ composite abutments for dental implant. *Journal of Biomedical Materials Research.* 2000;53(4):438-443.

KIM, S. S., YEO, I. S., LEE, S. J., KIM, D. J., JANG, B. M., KIM, S. H. & HAN, J. S. Clinical use of alumina-toughened zirconia abutments for implant-supported restoration: prospective cohort study of survival analysis. *Clinical Oral Implants Research*. 2013;24(5):517-522.

KIRSCH, C., ENDER, A., ATTIN, T. & MEHL, A. Trueness of four different milling procedures used in dental CAD/CAM systems. *Clinical Oral Investigations*. 2017;21(2):551-558.

KOLAKARNPRASERT, N., KAIZER, M. R., KIM, D. K. & ZHANG, Y. New multi-layered zirconias: Composition, microstructure and translucency. *Dental Materials*. 2019;35(5):797-806.

LANG, N. P., KIEL, R. A. & ANDERHALDEN, K. Clinical and microbiological effects of subgingival restorations with overhanging or clinically perfect margins. *Journal of Clinical Periodontology*. 1983;10(6):563-578.

LERNER, H., NAGY, K., PRANNO, N., ZARONE, F., ADMAKIN, O. & MANGANO, F. Trueness and precision of 3D-printed versus milled monolithic zirconia crowns: An in vitro study. *Journal of Dentistry*.

2021;113:103792.

LI, R., CHEN, H., WANG, Y. & SUN, Y. Performance of stereolithography and milling in fabricating monolithic zirconia crowns with different finish line designs. *Journal of the Mechanical Behavior of Biomedical Materials*. 2021;115: 104255.

LIU, S. Y. & CHEN, I. W. Fatigue of yttria-stabilized zirconia: I, fatigue damage, fracture origins, and lifetime prediction. *Journal of the American Ceramic Society*. 1991;74(6):1197-1205.

LüMKEMANN, N. & STAWARCZYK, B. Impact of hydrothermal aging on the light transmittance and flexural strength of colored yttria-stabilized zirconia materials of different formulations. *The Journal of Prosthetic Dentistry*. 2021;125(3):518-526.

MALKONDU, Ö., TINASTEPE, N., AKAN, E. & KAZAZOĞLU, E. An overview of monolithic zirconia in dentistry. *Biotechnology & Biotechnological Equipment*. 2016;30(4):644-652.

MEHL, A., REICH, S., BEUER, F. & GüTH, J. F. Accuracy, trueness, and precision—A guideline for evaluation of these basic values in digital dentistry. *International Journal of Computerized Dentistry*. 2021;24:341-352.

MICHAILOVA, M., ELSAYED, A., FABEL, G., EDELHOFF, D., ZYLLA, I. M. & STAWARCZYK, B. Comparison between novel strength-gradient and color-gradient multilayered zirconia using conventional and high-speed sintering. *Journal of the Mechanical Behavior of Biomedical Materials*. 2020;111:103977.

MIYAZAKI, T., NAKAMURA, T., MATSUMURA, H., BAN, S. & KOBAYASHI,

T. Current status of zirconia restoration. *Journal of Prosthodontic Research*. 2013;57(4):236-261.

NAKAMURA, K., HARADA, A., INAGAKI, R., KANNO, T., NIWANO, Y., MILLEDING, P. & ÖRTENGREN, U. Fracture resistance of monolithic zirconia molar crowns with reduced thickness. *Acta Odontologica Scandinavica*. 2015;73(8):602-608.

NAKAMURA, T., NAKANO, Y., USAMI, H., OKAMURA, S., WAKABAYASHI, K. & YATANI, H. In vitro investigation of fracture load and aging resistance of high-speed sintered monolithic tooth-borne zirconia crowns. *Journal of Prosthodontic Research*. 2020;64(2):182-187.

OH, W. S., DELONG, R. & ANUSAVICE, K. J. Factors affecting enamel and ceramic wear: a literature review. *The Journal of Prosthetic Dentistry*. 2002;87(4):451-459.

PEREIRA, G. K., GUILARDI, L. F., DAPIEVE, K. S., KLEVERLAAN, C. J., RIPPE, M. P. & VALANDRO, L. F. Mechanical reliability, fatigue strength and survival analysis of new polycrystalline translucent zirconia ceramics for monolithic restorations. *Journal of the Mechanical Behavior of Biomedical Materials*. 2018;85:57-65.

PYO, S. W., KIM, D. J., HAN, J. S. & YEO, I. S. L. Ceramic materials and technologies applied to digital works in implant-supported restorative dentistry. *Materials*. 2020;13(8):1964.

REKOW, D. & THOMPSON, V. Near-surface damage-a persistent problem in crowns obtained by computer-aided design and manufacturing. *Proceedings of the Institution of Mechanical Engineers, Part H*. 2005;219(4):233-243.

REVILLA-LEóN, M., HUSAIN, N. A. H., CEBALLOS, L. & ÖZCAN, M. Flexural strength and Weibull characteristics of stereolithography additive manufactured versus milled zirconia. *The Journal of Prosthetic Dentistry*. 2021;125(4): 685-690.

REVILLA-LEóN, M., METHANI, M. M., MORTON, D. & ZANDINEJAD, A. Internal and marginal discrepancies associated with stereolithography (SLA) additively manufactured zirconia crowns. *The Journal of Prosthetic Dentistry*. 2020;124(6):730-737.

REZENDE, C. E. E., BORGES, A. F. S., MACEDO, R. M., RUBO, J. H. & GRIGGS, J. A. Dimensional changes from the sintering process and fit of Y-TZP copings: Micro-CT analysis. *Dental Materials*. 2017;33(11):e405-e413.

SAILER, I., FEHéR, A., FILSER, F., GAUCKLER, L. J., LüTHY, H. & HäMMERLE, C. H. F. Five-year clinical results of zirconia frameworks for posterior fixed partial dentures. *International Journal of Prosthodontics*. 2007;20(4):383-388.

SCHERRE, S. & DE RIJK, W. G. The effect of crown length on the fracture resistance of posterior porcelain and glass-ceramic crowns. *International Journal of Prosthodontics*. 1992;5(6): 550-557.

SCHERRER, S. & DE RIJK, W. The fracture resistance of all-ceramic crowns on supporting structures with different elastic moduli. *International Journal of Prosthodontics*. 1993;6(5):462-467.

SCHRIWER, C., SKJOLD, A., GJERDET, N. R. & ØILO, M. Monolithic zirconia dental crowns. Internal fit, margin quality, fracture mode and load at fracture. *Dental Materials*. 2017;33(9):1012-1020.

SCHUBERT, H. & FREY, F. Stability of Y-TZP during hydrothermal treatment: neutron experiments and stability considerations. *Journal of the European Ceramic Society*. 2005;25(9):1597-1602.

SCHWENTENWEIN, M. & HOMA, J. Additive manufacturing of dense alumina ceramics. *International Journal of Applied Ceramic Technology*. 2015;12(1):1-7.

SON, K., LEE, J. H. & LEE, K. B. Comparison of intaglio surface trueness of interim dental crowns fabricated with SLA 3D printing, DLP 3D printing, and milling technologies. *Healthcare*. 2021;9(8):983.

STAWARCZYK, B., KEUL, C., EICHBERGER, M., FIGGE, D., EDELHOFF, D. & LüMKEMANN, N. Three generations of zirconia: From veneered to monolithic. Part I. *Quintessence International*. 2017;48(5):369-380.

STAWARCZYK, B., ÖZCAN, M., HALLMANN, L., ENDER, A., MEHL, A. & HæMMERLET, C. H. The effect of zirconia sintering temperature on flexural strength, grain size, and contrast ratio. *Clinical Oral Investigations*. 2013;17(1):269-274.

STEINER, M., MITSIAS, M. E., LUDWIG, K. & KERN, M. In vitro evaluation of a mechanical testing chewing simulator. *Dental Materials*. 2009;25(4):494-499.

STRUB, J. R., REKOW, E. D. & WITKOWSKI, S. Computer-aided design and fabrication of dental restorations: current systems and future possibilities. *The Journal of the American Dental Association*. 2006;137(9):1289-1296.

TINSCHERTA, J., NATTB, G., HASSENPFLUGB, S. & SPIEKERMANNA, H. Status of Current CAD/CAM Technology in Dental Medicine Stand der aktuellen CAD/CAM-Technik in der Zahnmedizin. *International Journal*

*of Computerized Dentistry*. 2004;7:25-45.

TORABI, K., FARJOOD, E. & HAMEDANI, S. Rapid prototyping technologies and their applications in prosthodontics, a review of literature. *Journal of Dentistry*. 2015;16(1):1-9.

VAN NOORT, R. The future of dental devices is digital. *Dental Materials*. 2012;28(1):3-12.

WANG, W. & SUN, J. Dimensional accuracy and clinical adaptation of ceramic crowns fabricated with the stereolithography technique. *The Journal of Prosthetic Dentistry*. 2021;125(4): 657-663.

WANG, W., YU, H., LIU, Y., JIANG, X. & GAO, B. Trueness analysis of zirconia crowns fabricated with 3-dimensional printing. *The Journal of Prosthetic Dentistry*. 2019;121(2):285-291.

WEI, C., GONG, X., XIE, C., CHEN, Z., LI, S. & GREMILLARD, L. In vitro cyclic fatigue and hydrothermal aging lifetime assessment of yttria-stabilized zirconia dental ceramics. *Journal of the European Ceramic Society*. 2020;40(13):4647 -4654.

WEI, C. & GREMILLARD, L. Towards the prediction of hydrothermal ageing of 3Y-TZP bioceramics from processing parameters. *Acta Materialia*. 2018;144:245-256.

WHITE, S., MIKLUS, V., MCLAREN, E., LANG, L. & CAPUTO, A. Flexural strength of a layered zirconia and porcelain dental all-ceramic system. *The Journal of Prosthetic Dentistry*. 2005;94(2):125-131.

WIEDENMANN, F., PFEFFERLE, R., REICHERT, A., JERMAN, E. & STAWARCZYK, B. Impact of high-speed sintering, layer thickness and artificial aging on the fracture load and two-body wear of zirconia crowns.

*Dental Materials*. 2020; 36(7):846-853.

WISKOTT, H. W., NICHOLLS, J. I., BELSER, U. C., WISKOTT, H., NICHOLLS, J. & BELSER, U. Stress fatigue: basic principles and prosthodontic implications. *International Journal of Prosthodontics*. 1995;8(2):105-116

ZHANG, F., INOKOSHI, M., BATUK, M., HADERMANN, J., NAERT, I., VAN MEERBEEK, B. & VLEUGELS, J. Strength, toughness and aging stability of highly-translucent Y-TZP ceramics for dental restorations. *Dental Materials*. 2016; 32(12):e327-e337.

# TABLES

**Table 1.** Parameters for artificial aging used in this study

| Transverse path | Speed (mm/s) | Weight | Thermal cycling | Cycle |
|---|---|---|---|---|
| Downward: 2 mm<br>Lateral: 0.7 mm | Up: 55<br>Down: 30<br>Forward: 30<br>Back: 55 | 5 kg | Temperature: 5℃–55℃<br>Dwell time: 60 s | Number: 120,000<br>Frequency: 1.5 Hz |

**Table 2.** Intaglio trueness (μm, root-mean-square estimates, mean ± standard deviation) of seven different zirconia crown groups measured in four areas of inspection

| Area | Groups | | | | | | |
|---|---|---|---|---|---|---|---|
| | ADZ | ASZ | FSZ | C4Z | S4Z | C5Z | S5Z |
| Inner surface | 32.57 ± 1.30 | 34.81 ± 1.80 | 33.72 ± 2.35 | 30.76 ± 9.11 | 26.94 ± 5.91 | 29.76 ± 3.63 | 29.56 ± 4.51 |
| Margin | 54.20 ± 5.18 | 62.39 ± 3.08 | 37.96 ± 3.83 | 30.91 ± 6.09 | 28.71 ± 6.30 | 34.80 ± 8.85 | 29.16 ± 4.66 |
| Occlusal | 19.47 ± 3.33 | 27.05 ± 2.49 | 29.81 ± 4.46 | 23.87 ± 4.75 | 21.11 ± 2.97 | 21.59 ± 3.12 | 22.39 ± 3.68 |
| Axial | 25.11 ± 3.90 | 21.51 ± 4.19 | 36.69 ± 7.29 | 35.41 ±14.78 | 29.79 ± 9.85 | 32.07 ± 7.46 | 34.72 ± 7.21 |

**Table 3.** Fracture load (N) of the seven different zirconia crown groups

| Aging | Group | | | | | | |
|---|---|---|---|---|---|---|---|
| | ADZ | ASZ | FSZ | C4Z | S4Z | C5Z | S5Z |
| Non-aging | 11166.54 ±2034.16 | 8325.29 ± 1909.73 | 10945.85 ± 1897.82 | 7929.14 ± 1321.22 | 6720.43 ± 829.34 | 6334.08 ±1344.86 | 5329.84 ± 1061.87 |
| Aging | 8241.23 ± 2240.32 | 6355.13 ± 1928.39 | 10490.75 ± 1739.02 | 5335.25 ± 1637.95 | 4756.07 ± 1355.76 | 5077.29 ± 1333.02 | 4749.78 ± 1174.88 |

# FIGURES

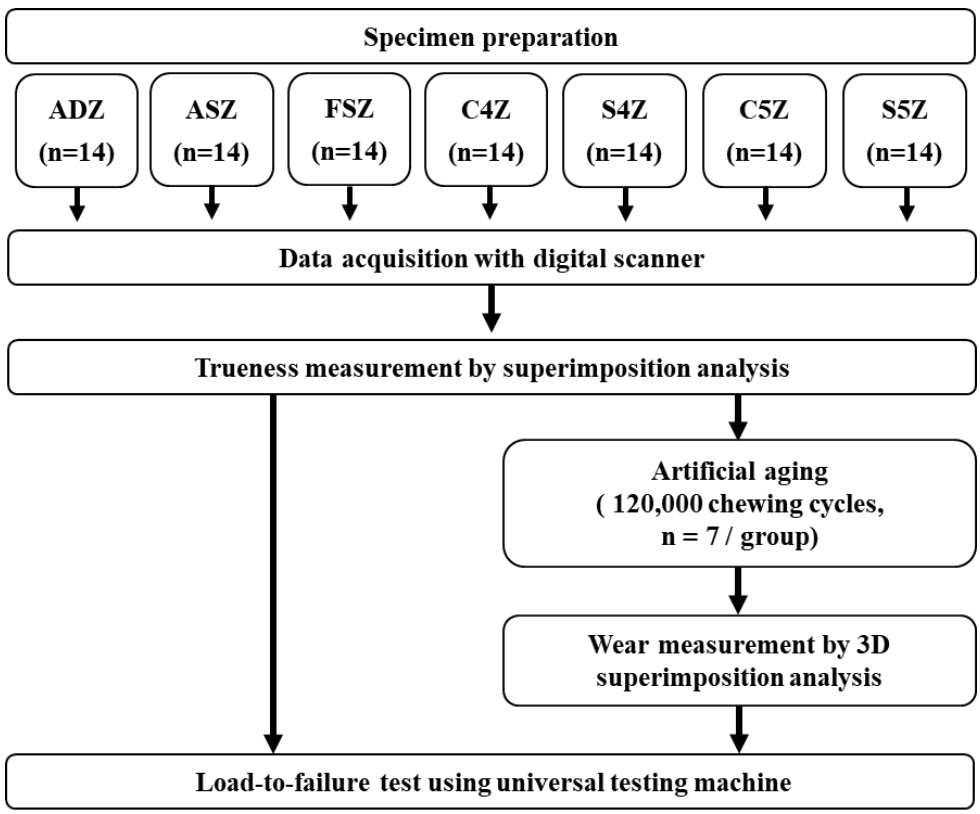


**Figure 1.** Flowchart of research.

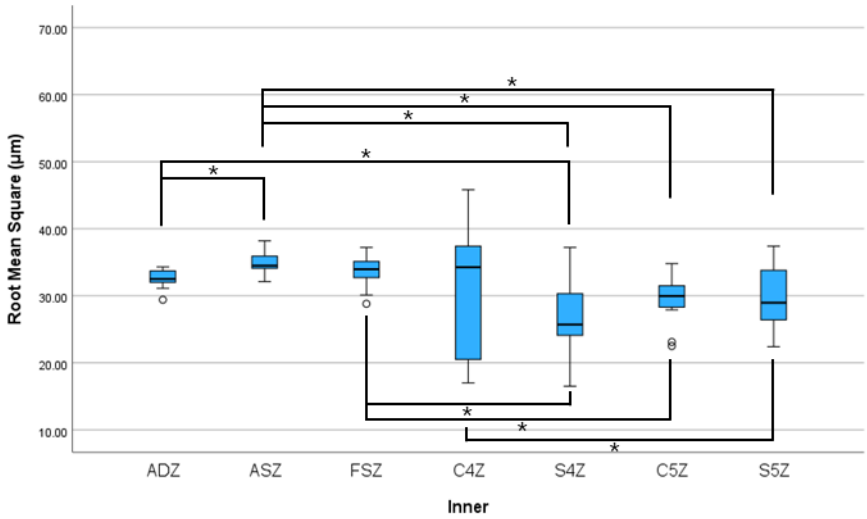
Root Mean Square (µm)
70.00
60.00
50.00
40.00
30.00
20.00
10.00
ADZ
ASZ
FSZ
C4Z
S4Z
C5Z
S5Z
Inner

(A)

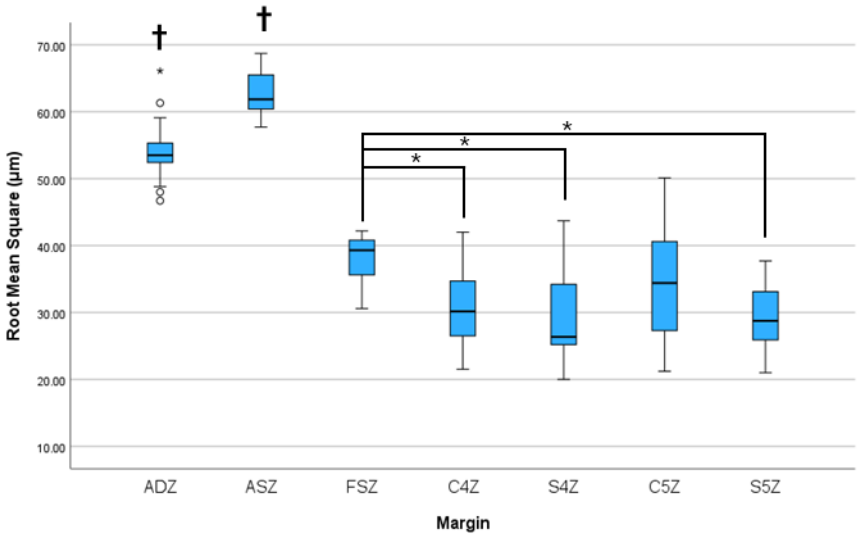
Root Mean Square (µm)
70.00
60.00
50.00
40.00
30.00
20.00
10.00
ADZ
ASZ
FSZ
C4Z
S4Z
C5Z
S5Z
Margin

(B)

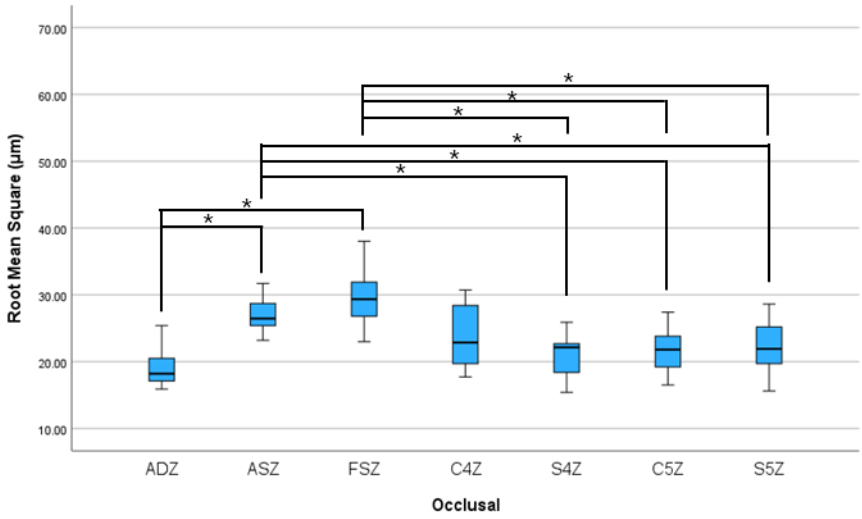


(C)

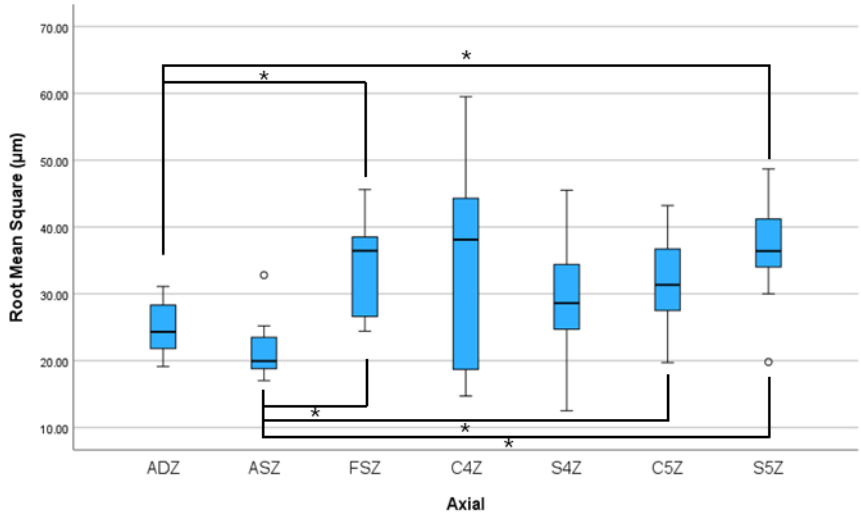


(D)

**Figure 2.** Intaglio surface trueness measurements (µm, root-mean-square) of seven zirconia groups in four different areas of inspection. (A) Inner surface area, (B) Margin area, (C) Occlusal area, (D) Axial area. A statistically significant difference ($p < 0.05$) was marked with an asterisk (*). Two groups marked with dagger (†) had statistical significance with the other five groups.

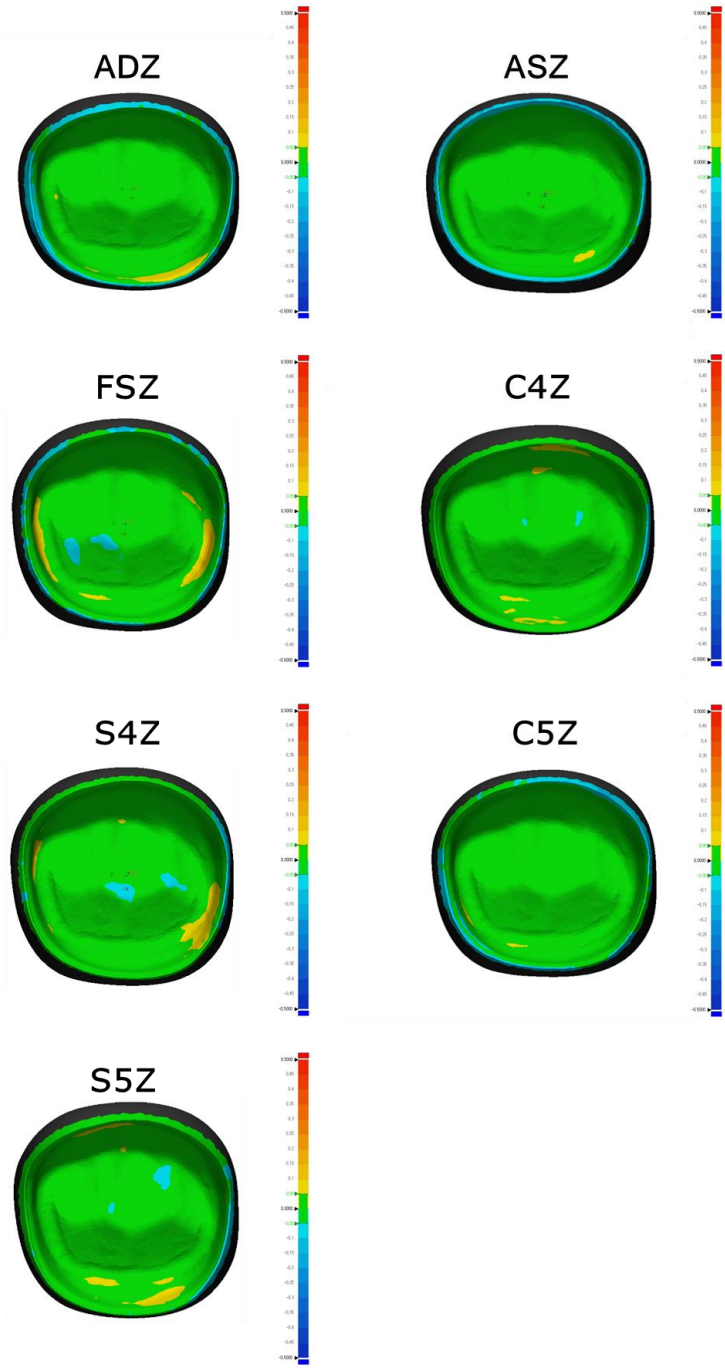


**Figure 3.** Representative color deviation maps of intaglio trueness of seven zirconia crown groups (positive deviation, yellow to red, negative deviation, cyan to blue, deviation below 50 μm, green).

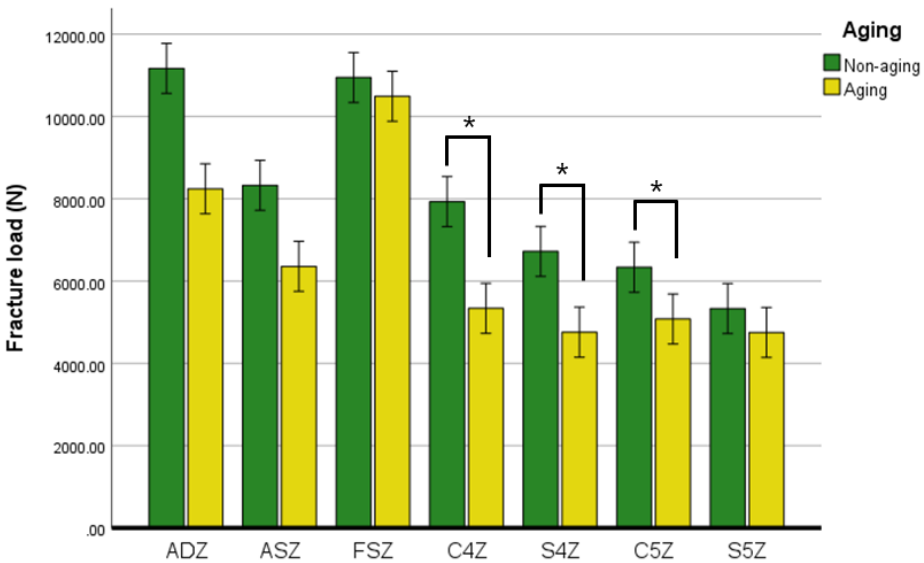


**Figure 4.** Fracture load of the seven zirconia groups. A statistically significant difference ($p < 0.05$) was marked with an asterisk (*).

# 국문 초록

# 제조 방식 및 재료에 따른 지르코니아 보철물의 전임상 비교 연구

서울대학교 대학원 치의과학과 치과보철학 전공

(지도교수 한 중 석)

김 용 규

1. 목 적

보철물 내면 적합도, 대합치 마모 및 파절 저항성을 비교하여 다양한 방식 및 재료로 제작된 지르코니아 크라운을 임상 적용 가능성을 확인하고자 한다.

2. 방 법

다음의 총 7개의 그룹에 대하여 그룹별로 14개씩 단일 구조 지르코니아 크라운 제작하였다. DLP와 SLA 방식의 서로 다른 3D printer로 적층 제작한 2 그룹(ADZ, ASZ), 완소결 지르코니아 블록 ((Y, Nb)-stabilized zirconia)을 절삭 가공하여 제작한 그룹(FSZ), 4 혹은 5 mol% yttria 안정화 반소결 지르코니아를 절삭 가공한 뒤 기존의 소성 혹은 고속 소성한 4 그룹(C4Z, S4Z, C5Z, S5Z)으로 총 7개의 그룹을

실험군으로 하였다. 각 그룹에 대하여 14개의 단일 구조 지르코니아 크라운 제작하였고, 이를 구강 스캐너로 스캔하였다. 3D inspection software을 이용하여 내면 전체, 교합면, 변연, 축면 4가지 영역에서 내면 적합도를 측정하였다. 각 그룹 별로 시편의 절반을 저작 시험기로 120,000 cycle의 저작 시험 시행하였고, 사람의 상악 대구치를 대합치로 이용하였다. 저작 시험 전, 후에 대합치를 모델 스캐너로 스캔한 뒤, 3D inspection software를 이용하여 마모된 부피를 측정하였다. 모든 시편을 universal testing machine을 이용하여 파절 시의 하중값을 측정하였다. 통계 분석을 위해 내면 적합도는 Welch's ANOVA, 대합치 마모량은 Kruskal-Wallis test, 그룹 및 aging의 영향은 two-way ANOVA를 통하여 분석하였다. 추가로 one-way ANOVA를 이용하여 aging 전과 후의 그룹간의 파절 하중의 차이를 분석하였고, paired t-test를 통해 각 그룹마다 파절 하중에 aging이 미치는 영향을 분석하였다.

3. 결 과

내면 전체에 대한 적합도는 그룹 간의 유의미한 차이가 있었으나 평균 RMS 값의 차이가 5.25 $\mu$m 이내였다. 적층 가공을 이용한 그룹들은 축과 교합면에서 높은 적합도와 낮은 편차를 보였으나, 변연부에서는 낮은 적합도를 보였다. 변연에서 낮은 적합도를 보였고, 반소결 지르코니아를 이용한 그룹들은 축면에서 낮은 적합도를 보였다. 완소결 지르코니아 그룹의 내면 재현성은 전반적으로 부분적으로 소결된 지르코니아 그룹보다 높았으나, 교합면과 변연에서 낮은 적합도를 보였다. 부분적으로 소결된 지르코니아 그룹은 축면에서 낮은 적합도를 보이고, 동일한 부분적으로 소결된 지르코니아 블록에서 고속 소성으로 인한 적합도의 유의미한 차이는 없었다. 저작 시험 동안 지르코니아 파절은 관찰되지 않았고, 지르코니아의 마모량은 매우 적었다. 대합되는 자연치의 마모량은

Kruskal-Wallis test를 통해 그룹 간 유의한 차이가 없다고 밝혀졌다. ($p = 0.808$). 파절 하중값을 보면, Two-way ANOVA를 통해 그룹과 aging이 하중값에 유의미한 영향을 미치는 것을 알 수 있었고 (both, $p < 0.001$), 서로 간의 상호작용은 없었다. ($p = 0.301$). One-way ANOVA는 ADZ, FSZ 그룹이 다른 그룹에 비해 파절 하중값이 aging 전과 후에 모두 유의미하게 큰 값을 가짐을 나타냈고, paired t-test에서는 S4Z, C4Z, C5Z 그룹은 aging으로 인해 유의미한 감소를 보였다.

## 4. 결 론

적층 가공, 완소결 블록, 고속 소성을 이용하여 제작한 지르코니아 보철물은 기존 방식으로 제작된 보철물과 비교하여, 내면 적합도, 대합치 마모량, 파절 저항성 측면에서 임상에 적용 가능할 정도의 결과를 보였다.

---

주요어 : 지르코니아; 적층 가공; 완소결 지르코니아; 고속 소성; 내면 적합도; 파절 저항성; 저작 시험;

학번 : 2019-39896